Clim. Past Discuss., 9, 6459–6494, 2013
www.clim-past-discuss.net/9/6459/2013/
doi:10.5194/cpd-9-6459-2013

Climate of the Past Discussions
Open Access

Extreme warming, photic zone euxinia and sea level rise during the Paleocene/Eocene Thermal Maximum on the Gulf of Mexico Coastal Plain; connecting marginal marine biotic signals, nutrient cycling and ocean deoxygenation

A. Sluijs[1], L. van Roij[1], G. J. Harrington[2], S. Schouten[1,3], J. A. Sessa[4,5], L. J. LeVay[5,6], G.-J. Reichart[1], and C. P. Slomp[1]

[1]Department of Earth Sciences, Faculty of Geosciences, Utrecht University, Budapestlaan 4, 3584CD Utrecht, the Netherlands
[2]School of Geography, Earth and Environmental Sciences, Aston Webb Building, University of Birmingham, Birmingham, B15 2TT, UK
[3]NIOZ Royal Netherlands Institute for Sea Research, Department of Marine Organic Biogeochemistry, P.O. Box 59, 1790 AB Den Burg, Texel, the Netherlands

[4]Department of Paleontology, American Museum of Natural History, Central Park West at 79th St., New York, NY 10024, USA
[5]Department of Geosciences, Pennsylvania State University, University Park, PA 16802, USA
[6]International Ocean Discovery Program and Department of Geology and Geophysics, Texas A&M University, College Station, Texas, 77845, USA

Received: 8 November 2013 – Accepted: 15 November 2013 – Published: 3 December 2013

Correspondence to: A. Sluijs (a.sluijs@uu.nl)

Published by Copernicus Publications on behalf of the European Geosciences Union.

CPD
9, 6459–6494, 2013

Abstract

The Paleocene/Eocene Thermal Maximum (PETM, ~56 Ma) was a ~200 kyr episode of global warming, associated with massive injections of ^{13}C-depleted carbon into the ocean-atmosphere system. Although climate change during the PETM is relatively well constrained, effects on marine oxygen and nutrient cycling remain largely unclear. We identify the PETM in a sediment core from the US margin of the Gulf of Mexico. Biomarker-based paleotemperature proxies (MBT/CBT and TEX_{86}) indicate that continental air and sea surface temperatures warmed from 27–29 °C to ~35 °C, although variations in the relative abundances of terrestrial and marine biomarkers may have influenced the record. Vegetation changes as recorded from pollen assemblages supports profound warming.

Lithology, relative abundances of terrestrial vs. marine palynomorphs as well as dinoflagellate cyst and biomarker assemblages indicate sea level rise during the PETM, consistent with previously recognized eustatic rise. The recognition of a maximum flooding surface during the PETM changes regional sequence stratigraphic interpretations, which allows us to exclude the previously posed hypothesis that a nearby fossil found in PETM-deposits represents the first North American primate.

Within the PETM we record the biomarker isorenieratane, diagnostic of euxinic photic zone conditions. A global data compilation indicates that deoxygenation occurred in large regions of the global ocean in response to warming, hydrological change, and carbon cycle feedbacks, particularly along continental margins, analogous to modern trends. Seafloor deoxygenation and widespread anoxia likely caused phosphorus regeneration from suboxic and anoxic sediments. We argue that this fuelled shelf eutrophication, as widely recorded from microfossil studies, increasing organic carbon burial along continental margins as a negative feedback to carbon input and global warming. If properly quantified with future work, the PETM offers the opportunity to assess the biogeochemical effects of enhanced phosphorus regeneration, as well as

CPD
9, 6459–6494, 2013

the time-scales on which this feedback operates in view of modern and future ocean deoxygenation.

1 Introduction

The Paleocene-Eocene Thermal maximum (PETM; ∼ 56 Ma) is one of at least three geologically brief (< 200 kyr) global warming events, often referred to as "hyperthermals" (Thomas and Zachos, 2000), superimposed on a long-term late Paleocene – early Eocene warming trend (Zachos et al., 2008). The PETM is marked by a ∼ 2–7 ‰ negative carbon isotope excursion (CIE), recorded in marine and terrestrial sedimentary components, and carbonate dissolution in deep-sea sediment records (Sluijs et al., 2007a). These phenomena indicate a massive injection of ^{13}C-depleted carbon into the ocean-atmosphere system, but the mechanism for this release remains controversial (Dickens, 2011). Although coverage for low latitude regions is limited, the available information suggests that the global average surface temperature warmed by 4–5 °C (Kennett and Stott, 1991; Zachos et al., 2003; Sluijs et al., 2006; Dunkley Jones et al., 2013). A rise in sea level has been recorded along several mid- to high latitude continental margins, suggesting eustatic rise (Sluijs et al., 2008a).

The PETM is characterized by major biotic response, including global dominance of the dinoflagellate *Apectodinium* and the extinction of ∼ 50 % of the deep-sea benthic foraminifera species (Sluijs et al., 2007a). Moreover, the PETM is globally recognized as a major catalyst in mammal migration and evolution, including the first and widespread occurrence of primates (Bowen et al., 2002). The causes of biotic change, notably for the marine realm, remain largely uncertain (Gibbs et al., 2012). One of the proposed forcing mechanisms for marine biotic change has been deoxygenation (Thomas, 2004), as several studies have presented evidence of a decrease in water column oxygen content in deep, intermediate and shallow settings, although the full extent and consequences remain unclear (Speijer and Wagner, 2002; Sluijs et al., 2006; Dickson et al., 2012).

CPD
9, 6459–6494, 2013

Previous work has attempted to locate the PETM in sediment sequences along the US Gulf Coastal Plain (GCP; Fig. 1) (e.g., Harrington et al., 2004; Beard, 2008) A channel sand that may represent the early stages of the PETM near Meridian, Mississippi, and a subsequent hiatus has been attributed to sea level drop during the PETM (Beard, 2008). A primate fossil found within this channel sand was therefore hypothesized to be the oldest North American primate on record, leading to revised migrational patterns of these early primates (Beard, 2008). Here, we present a multi-proxy stratigraphic, paleoecologic and paleoclimatologic study of late Paleocene and early Eocene sediments recovered in the Harrell Core, close to Meridian, Mississippi, USA (Harrington et al., 2004), deposited at $\sim 28^{\circ}$ N paleolatitude (Müller et al., 2009) (Fig. 1). We analyzed physical sediment properties, organic matter (bulk and compound specific) carbon isotope ratios, palynology (dinoflagellate cysts, pollen and spores), and calcareous nannofossils to document climate change and ocean oxygenation at these times. The first identification of the PETM at the GCP and documentation of sea surface and continental warming has regional implications for stratigraphy and primate migration patterns. Moreover, these new data, combined with an extensive data compilation, suggest that ocean deoxygenation played a major role in nutrient cycling, biotic changes and carbon cycle evolution during the PETM.

2 Regional stratigraphy and material

The stratigraphy and depositional environments of the Tuscahoma and Hatchetigbee formations from the eastern Gulf Coastal Plain (GCP; Mississippi through Georgia; Fig. S1 in the Supplement) have been the subject of multidisciplinary study of pollen (Tschudy, 1973; Frederiksen, 1998; Harrington, 2001, 2003; Harrington and Jaramillo, 2007), plants (Danehy et al., 2007), mammals (Beard and Dawson, 2001; Beard, 2008), dinoflagellate cysts (Edwards and Guex, 1996), planktonic foraminifera (Mancini, 1981; Mancini and Oliver, 1981), calcareous nannoplankton (Gibson et al., 1982; Gibson and Bybell, 1994), mollusks (Sessa et al., 2012a), magnetostratigraphy

CPD
9, 6459–6494, 2013

(Rhodes et al., 1999) and sequence stratigraphy (Mancini and Tew, 1995); see Sessa et al. (2012b) for an overview. Hence, the stratigraphy of the GCP in Mississippi is well-understood, although the PETM was never positively identified using carbon isotope stratigraphy. The Tuscahoma Fm, the uppermost part of the middle Wilcox Group, underlies the Hatchetigbee Fm, which is the basal unit of the upper Wilcox Group (Tschudy, 1973). The Bashi Marl Member lies, locally within parts of Mississippi and Alabama, at the base of the Hatchetigbee Fm. The depositional environments of the eastern GCP during the latest Paleocene and earliest Eocene were very shallow marine settings that periodically became emergent and formed swamps that are now preserved locally as lignites (Mancini, 1981; Mancini and Oliver, 1981; Gibson et al., 1982). The Bashi depositional environments were more marine than those of the Tuscahoma and contain calcareous fossils (Gibson et al., 1982). The Bashi Marl is still, however, shallow marine with an estimated water depth of much less than 50 m in Meridian, Mississippi (Sessa et al., 2012b).

We sampled the Tuscahoma Formation and Bashi Member recovered in the Harrell Core, drilled close to Meridian, Mississippi, by the Mississippi Department of Environmental Quality, Office of Geology (Fig. 1). The upper portion of the Tuscahoma Formation (c. 80 m) within the Harrell Core from Meridian, Lauderdale Co, Mississippi (Fig. 1) lacks calcareous fossils and is typified by excellent pollen yields from both lignites and clastic lithologies (Harrington et al., 2004; Harrington and Jaramillo, 2007).

3 Methods

Smear slides were made for calcareous nannofossil analyses. Then, samples were freeze-dried and splits were analyzed for total magnetic susceptibility, palynology and organic geochemistry. Magnetic susceptibility per gram of sediment (MS) was measured using the AGICO KLY-3 device at Utrecht University. Standard palynological treatment was applied for dinocysts and pollen and spore analyses. For the analyses of dinocysts and ratios of marine vs. terrestrial palynomorphs, freeze-dried sediment was

CPD
9, 6459–6494, 2013

treated with 30 % HCl and twice with 38 % HF and sieved over a 15-µm nylon mesh. Residues were analyzed at > 500 × magnification. See Supplement for a taxonomical section. Materials are stored in the collection of the Laboratory of Palaeobotany and Palynology, at Utrecht University. For pollen and spore analyses, approximately 15 grams of sediment was ground in a mortar with pestle and then soaked overnight in HCl to remove any carbonate. These samples were then treated with 40 % HF and left for 3 days to digest silicate minerals before sieving with a 10-µm mesh. Samples were then placed into hot HCl to remove any remaining precipitate before sieving once more with a 10 µm mesh. The final stage to remove excess organic matter and any pyrite was to wash the samples in concentrated HNO_3 for 2 min before a final iteration of sieving. Samples were stained with safranin and then mounted onto coverslips and analyzed at 400x and 1000x phase contrast magnification.

All $\delta^{13}C$ analyses on total organic carbon (TOC) were performed on decarbonated, freeze-dried samples with a Fison NA 1500 CNS analyzer, connected to a Finnigan Delta Plus mass spectrometer. Analytical precision was better than 0.1 ‰. All values are reported relative to the VPDB standard.

For biomarker analyses, powdered and freeze-dried sediments were extracted with a Dionex Accelerated Solvent Extractor using a 9 : 1 (v/v) mixture of dichloromethane and methanol. One aliquot of the extract was separated into apolar and polar fractions. Polar fractions were analyzed using high-performance liquid chromatography/atmospheric pressure chemical ionization-mass spectrometry (Schouten et al., 2007) using an Agilent 1100 HPLC-MSD SL. Single-ion monitoring was used to quantify the abundance of glycerol dialkyl glycerol tetraethers (GDGTs). We apply the TEX_{86}^{H} SST core top calibration which has a calibration error of 2.5 °C, as this is recommended for (sub)tropical oceans (Kim et al., 2010). We have also calculated TEX_{86}^{L} values following a recent suggestion that this calibration may provide more realistic results for shallow marine sections (Taylor et al., 2013).

The distribution of the branched GDGTs, produced by soil bacteria, is a measure for mean annual air temperature (MAAT) using the MBT/CBT proxy (Weijers et al., 2007).

CPD
9, 6459–6494, 2013

We applied both the MBT/CBT calibration of Weijers et al. (2007) and the MBT'/CBT of Peterse et al. (2012) calibration, which yield calibration errors of ~5 °C. We also determined the abundances of the branched relative to the isoprenoid tetraethers (BIT index), a proxy for the amount of river derived soil organic matter vs. marine organic matter (Hopmans et al., 2004). Another aliquot of the total extract was desulfurized using Raney nickel (Sinninghe Damsté et al., 1988) and subsequently separated into polar and apolar fractions. Apolar fractions were hydrogenated using PtO_2/H_2 and analyzed by gas chromatography (Agilent 6890), gas chromatography/mass spectrometry (Thermofinnigan DSQ) and gas chromatography/isotope ratio mass spectrometry (Thermofinning Delta V coupled to an Agilent 6890).

All data are included in the Supplement.

4 Results and discussion

4.1 Stratigraphy of the Harrell Core

At ~121.9 m below surface (mbs), the $\delta^{13}C_{TOC}$ shows a negative step from average values of −25.5 ‰ ($1\sigma = 0.25$) to values averaging −27.5 ‰ ($1\sigma = 0.70$) up to 118.6 mbs, with minimum values of −28.6 ‰ (Fig. 2). Because this could reflect an increase in the relative abundance of marine organic matter compared to terrestrial organic matter (Sluijs and Dickens, 2012) we tested if this excursion is also present in specific biomarkers. Although the abundance of biomarkers was insufficient for isotope analyses in many samples, particularly below 121.9 mbs, and results are based on relatively low yields resulting in relatively high standard deviations for the measurements, we reproduce the shift towards lower $\delta^{13}C$ in both sulfur-bound phytane, derived from algal chlorophyll (Brassell et al., 1986; Schoon et al., 2011) and sulfur-bound C_{29} sterane, likely derived from algal C_{29} sterols (Volkman, 1986). Concomitantly, abundances of *Apectodinium* spp. increase from ~30 to 80 % of the dinocyst assemblage. Paleocene abundances should be considered rough estimates; samples are dominated by

CPD
9, 6459–6494, 2013

terrestrial material, which complicates robust quantitative dinocyst analyses (see below). At the same level, both the TEX_{86} and MBT/CBT paleothermometers (Fig. 2) as well as the influx of abundant pollen derived from thermophyllic plants (Fig. 3; see Sect. 3.3) record extreme warming. The combined information unambiguously shows the presence of a hyperthermal.

We can exclude that the CIE in the Harrell Core reflects any of the hyperthermals younger than that of the PETM because we find the calcareous nannofossils *Discoaster multiradiatus* in the overlying Bashi Formation (Supplement Table 1). The last occurrence of this taxon is in uppermost NP10, which predates Eocene Thermal Maximum 2 by ~ 200 kyr (Lourens et al., 2005), and confirms previous age assessments of the basal Bashi Fm (Gibson and Bybell, 1994; Mancini and Tew, 1995). The combined information indicates the presence of the PETM in the uppermost Tuscahoma Fm in the Harrell Core.

The $\delta^{13}C_{TOC}$ record exhibits significant variation within the CIE. A positive spike in $\delta^{13}C_{TOC}$ occurs within the PETM at ~ 120.5 mbs. In part, this can be explained by an increase in the relative abundance of terrestrial organic matter (Sluijs and Dickens, 2012) as indicated by a concomitant increase in BIT index values, suggesting elevated input of soil organic matter, and abundances of terrestrial palynomorphs (Fig. 2, see below). This interval is rich in siliciclastic sand and mica and relatively poor in TOC, so that enhanced degradation of marine organic matter might have increased $\delta^{13}C_{TOC}$ values as well as BIT index values (Huguet et al., 2008). This might be due to either a time interval of non-deposition or erosion or, given the high abundances of terrestrial organic matter and the coarse grains, a storm deposit.

A ~ 10 cm thick sand-rich and highly micaceous interval bearing mollusk shells (121.9–121.8 mbs) at the base of the CIE marks a distinct peak in magnetic susceptibility (MS), suggesting an unconformity (Fig. 2). Constraints on the time associated with the hiatus are limited since the Tuscahoma Fm is poor in age-diagnostic fossils. However, regionally, notably in Western Alabama, approximately 60 m below the top of the Tuscahoma Fm is Bells Landing Marl, which has good biostratigraphic age constraints

CPD
9, 6459–6494, 2013

(Mancini and Tew, 1995). The presence of the planktonic foraminifer *Morozovella subbotinae, M. occlusa* (Mancini and Oliver, 1981; Mancini, 1984) indicates Bells Landing to rest within zone P5 of Wade et al. (2011). The presencse of the calcareous nannofossils *Discoaster mohleri* and *D. multiradiatus* (Gibson et al., 1982; Siesser, 1983) indicate zone NP9 of Martini (1971). The combined information implies a maximum age 900 kyr older than the PETM (Wade et al., 2011; Vandenberghe et al., 2012), which is hence a maximum duration of this hiatus. However, the onset of the PETM occurs also within P5 and NP9, implying that the minimum possible duration of the hiatus is negligible. Notably, *Globanomalina pseudomenardii* is absent from the Bells Landing Marl (Mancini, 1984), suggesting that it represents the upper part of zone P5 (Wade et al., 2011).

At Harrell, the depth of the Bells Landing Marl has not been determined. However, if also 60 m of sediment separates the Bells Landing Marl and the CIE by regional analogy, we suspect that the hiatus at the base of the PETM is minor. Indeed, a previous pollen study recorded long-term warming over this part of the section (Harrington and Jaramillo, 2007), consistent with other climate records during the last hundreds of thousands of years during Paleocene (Zachos et al., 2008; Bijl et al., 2009), suggesting that the sediment sequence represents a relatively complete latest Paleocene succession. The hiatus thus represents certainly much less than 1 million year and more likely in the order of or less than 100 kyr. This implies that the section is suitable to quantify the warming and environmental change during the PETM.

The top of the CIE corresponds to a sea level drop in MS and the Tuscahoma–Bashi contact. This boundary is marked by a widely recognized regional unconformity on the GCP (Gibson and Bybell, 1994). None of the records indicate the presence of the recovery interval, implying that the PETM is only partly present in the Harrell Core. The sediments were likely deposited during the first part (or *body*) of the PETM (~ 80 kyr) (Sluijs et al., 2007a), but the entire recovery interval was truncated by the upper sequence boundary. It remains unclear which portion of the first 80 kyr of the CIE is present. However, the high glauconite content, regardless whether it was produced

CPD
9, 6459–6494, 2013

in situ or transported (detailed analyses have not been performed), strongly suggests low sediment accumulation rates. This is supported by high dinoflagellate cyst concentrations (10^4–10^5 per gram of sediment, Supplement), suggesting accumulation on geological time scales rather than within centuries or millennia. This implies that sufficient time to record maximum PETM conditions is represented in the record.

4.2 Temperature

Both the TEX_{86} and MBT/CBT paleothermometers show a marked warming across the onset of the PETM, of 6 and 5–8 °C, respectively (Fig. 2). We calculated SSTs from isoprenoid GDGTs using various TEX_{86} calibrations (Supplement 1). We prefer the TEX_{86}^{H} SST core top calibration which has a calibration error of 2.5 °C, as this is recommended for (sub)tropical oceans (Kim et al., 2010). Despite the recent suggestion that TEX_{86}^{L} may better represent marginal marine regions (Taylor et al., 2013), this calibration results in unrealistically low SSTs of ~ 15 °C in the Paleocene and ~ 25 °C during the PETM (see Supplement) and are therefore not further considered. TEX_{86}^{H} indicates late Paleocene SSTs averaging 29 °C (1σ = 1.2), slightly higher than mean estimates based on mollusk geochemistry from the lower Eocene Bashi Fm of the GCP (Sessa et al., 2012b), and ~ 5 °C warmer than modern SSTs in this region. However, absolute temperature estimates based on TEX_{86} may be compromised due to the large supply of soil ether lipids, as indicated by high BIT values (Weijers et al., 2006). In this interval, higher BIT values correspond to relatively low TEX_{86} values (R^2 = 0.69), suggesting that SSTs could be underestimated.

Based on MBT/CBT, upper Paleocene mean annual air temperatures (MAAT) were 26.4 °C (1σ = 0.8) and 21.4 °C (1σ = 0.5) following the Weijers et al. (2007) and Peterse et al. (2012) calibrations, respectively (Fig. 2). Such temperatures agree with the tropical-pantropical character of the vegetation as recorded from plant macrofossils near the Tuscahoma–Bashi transition (Danehy et al., 2007). Quantitatively, the MAAT estimate based on the Weijers calibration corresponds remarkably well to estimates

CPD
9, 6459–6494, 2013

based on plant leaves (27 °C, Wolfe and Dilcher, 2000). Given the relatively large uncertainty in estimating absolute temperatures in both proxies, even the MAATs implied by the Peterse et al. (2012) calibration is within error of the leaf-based estimate. However, we consider the MAATs estimate from the Weijers et al. (2007) calibration to be more realistic for this area and time interval, also because they are much closer to SSTs as reconstructed from biomarkers and mollusk geochemistry from the region (Keating-Bitonti et al., 2011).

Average PETM TEX_{86} temperatures were 35 °C ($1\sigma = 0.7$). This implies a PETM warming of 6 °C, or slightly less given the potential bias towards lower values in the upper Paleocene due to the contribution of soil GDGTs (see above). MAAT rose by ~ 7–8 to 35 °C ($1\sigma = 1.4$) based on the Weijers et al. (2007) calibration and by ~ 5 to 26.6 °C ($1\sigma = 0.9$) following the Peterse et al. (2012) calibration. Because of the low relative abundances of terrestrial lipids in these sediments (indicated by low BIT index values) there is some uncertainty in absolute MBT/CBT temperature estimates due to potential in situ production of the lipids used in the MBT proxy (Peterse et al., 2009). Still, recent regional climate modeling experiments indicated that mean annual SSTs should be similar to MAAT along the GCP margin during this time period (Thrasher and Sloan, 2009), which is consistent with our data. Hence, considering that both proxies yield significant uncertainties in the present, the magnitude of MAAT and SST warming was likely in the order of 4–8 °C.

Proxy records of continental air and sea surface temperature across the late Paleocene to the first ~ 80 kyr of the PETM are available from at least 10 locations. These sites are spread across the globe, and all indicate a 4 to 8 °C warming (Fig. 4), the global average being close to 4–5 °C (Dunkley Jones et al., 2013). Deep ocean temperatures increased by a similar amount (Thomas and Shackleton, 1996; McCarren et al., 2009). Although records from tropical regions are rare, there is no evidence for polar amplification of warming and only little spatial variability in temperature trends. This suggests relatively little change in global atmospheric and oceanic circulation patterns and ocean-atmosphere heat transport during the PETM. In addition, absolute

CPD
9, 6459–6494, 2013

temperatures reconstructed here are relatively modest as compared to other mid and high latitude sites (Sluijs et al., 2006, 2011; Zachos et al., 2006; Dunkley Jones et al., 2013). Although more estimates from tropical regions are required, our data might be inconsistent with the recently proposed hypothesis (Huber and Caballero, 2011) put forth to explain extreme warmth at high latitudes, that low latitude regions were much warmer than previously anticipated. In their scenario, SSTs outside the PETM along the GCP should have been > 35 °C (Huber and Caballero, 2011) while all available data suggest temperatures well below 30 °C. Therefore, although uncertainties remain regarding the accuracy of the TEX_{86} and MBC/CBT proxies, our data may reinforce the notion that current climate theory (Huber and Caballero, 2011; Lunt et al., 2012) cannot yet fully explain the low meridional temperature gradients during the early Eocene and the PETM.

4.3 Terrestrial vegetation

A significant shift in palynofloral composition is recorded in the Harrell Core between 121.97 and 121.72 m: (i) changes in the relative abundance of range-through taxa, (ii) changes in the co-occurrence of taxa, (iii) the first occurrence of key Eocene marker taxa, and (iv) the presence of a transient flora with unique elements that are not observed at any time in the Paleocene or Eocene on the US Gulf Coast. These features are all consistent with an excursion flora observed in the Bighorn Basin of Wyoming (Wing et al., 2005; Wing and Currano, 2013).

The eight samples from the uppermost Tuscahoma Fm. (121.72 to 118.69 m) contain abundant palm pollen (*Arecipites, Proxapertites operculatus, P. psilatus,* and *Calmuspollenites eocenicus*) along with significant components of other monocots such as the *Sparganiaceae* (bur reeds). Below 121.72 m palm pollen averages 1 %, but from 121.72–118.69 m this increases to an average within-sample abundance of 13 % (Fig. 3a) which is statistically significant using a Mann–Whitney *U* test ($U_{77,8} = 0$, $p < 0.0001$). Gymnosperms of all groups decrease in abundance (Fig. 3a) or are absent, including the *Metasequioa/Glyptostrobus* pollen that is otherwise very abundant

CPD
9, 6459–6494, 2013

throughout many lower Paleogene pollen assemblages. This within-sample decrease during the PETM is statistically significant ($U_{77,8} = 48$, $p < 0.0001$). Juglandaceae pollen belonging to *Carya* (hickories) and *Momipites* is rare, although angiosperm pollen increases significantly within the PETM ($U_{77,8} = 16$, $p < 0.0001$) from 64 % in an average Paleocene sample to 85 % in a typical PETM sample (Fig. 3). This is also consistent with the pattern seen in Wyoming (Wing et al., 2005; McInerney and Wing, 2011). Increased abundance is recorded of *Porocolpopollenites ollivierae* (belonging the tropical families including Apocynaceae, Meliaceae or Styracaceae) together with many other taxa of unknown systematic affinity such as *Nudopollis terminalis* (a normapolles), *Thomsonipollis exploitus* (a normapolle but abundant) and different types of undescribed, new tricolporate pollen.

First occurrences include *Platycarya platycaryoides*, *Platycarya swasticoides, Interpollis microsupplingensis* and *Brosipollis* sp. that are all previously documented at the Red Hot Truck Stop (Harrington, 2003). In addition we record the first occurrence of *Ulmipollenites undulosus*, another feature of the Eocene (Frederiksen, 1998). Taxa that are considered to be transient include *Retistephanocolporites* that has only ever been recorded previously from the Red Hot Truck Stop (Harrington, 2003; plate 1, Fig. 32). Three common transient taxa are a large variety of *Milfordia* (member of the monocot Flagellariaceae, or Restoniaceae families), a type of *Ailanthipites* sp. that is large, clearly striate and not *Ailanthipites berryi,* and a very abundant type of tetracolporate, small striate/reticulate, oblate to spherical pollen grain that is not found anywhere else. There are other taxa that have first appearances within this interval, however, because they are not abundant they cannot be confidently considered as first (and only) occurrences. Several important taxa that are thought to go extinct at the Paleocene/Eocene boundary on the US Gulf Coast (Harrington, 2001; Harrington and Jaramillo, 2007) are not found in this interval (i.e., above 121.97 m) including *Holkopollenites chemardensis, Langiopollis cribellatus, L. lihokis,* and *Spineapollis spinata.*

There are significant differences between the PETM samples from 121.72–118.69 m in the Harrell Core and those immediately below in the upper Tuscahoma Formation

CPD
9, 6459–6494, 2013

as described by Harrington and Jaramillo (2007). We carried out non-metric multidimensional scaling ordination to illustrate relative abundance changes and presence-absence (top and bottom plots in Fig. 3b). For the relative abundance run, only taxa that contain 50 or more specimens within the whole dataset of the Harrell Core were included. These samples predominantly represent brackish water to very shallow marine environments and all lignites and carbonaceous shales have been removed from the Harrell sample set before ordination. Relative abundance changes reflect a decrease in Juglandaceae pollen, all gymnosperms, and myricaceous pollen and the increase of palms, other monocots and abundant transient taxa in the Eocene (Fig. S3A). The ordination of presence-absence data (Fig. S3B) reflects changes in co-occurrence patterns and the complete change of community membership in the uppermost Tuscahoma Fm. The latter ordination is run on taxa that contain 2 or more occurrences in 2 or more different samples and presence within a sample is recorded as "1" and absence as "0" regardless of the relative abundance within any particular sample.

4.4 Depositional environment and sea level

4.4.1 Upper Paleocene

Terrestrial palynomorphs (pollen and spores) comprise > 95 % of the palynomorphs in the uppermost Paleocene (125–121.9 mbs), cuticle fragments of terrestrial plant leaves are abundant, and BIT values are high (> 0.8). However, we recorded marine dinoflagellate cysts in all samples. As a result, quantification of assemblages is difficult. Dinocyst abundances in this interval are based on relatively low counts (between 10 and 60 cysts) and should therefore be considered as rough estimates. The assemblages in the Harrell core are typical for early Paleogene marginal marine deposits. Averaged over the entire interval (based on 238 cysts), *Apectodinium* spp. (27 %) and the *Senegalinium* complex (*sensu* Sluijs and Brinkhuis, 2009) (20 %) are abundant. The *Senegalinium* cpx. in the Harrell Core is almost exclusively comprised of *Senegalinium* spp., but includes sporadic *Phthanoperidinium* spp. and *Deflandrea*

CPD
9, 6459–6494, 2013

spp. The *Senegalinium* cpx., and *Senegalinium* spp., represents a group of taxa derived from dinoflagellates known to have been tolerant to low salinity waters, based on empirical information (Harland, 1973; Brinkhuis et al., 2006; Sluijs and Brinkhuis, 2009; Sluijs et al., 2009). Moreover, *Eocladopyxis* spp. are present and modern representatives of the family Goniodomidae are successful in very near shore and lagoonal settings, partly due to their euryhaline ecology (Zonneveld et al., 2013). Other consistently present dinocyst taxa include typical shelf taxa such as members of the *Cordosphaeridium fibrospinosum* cpx. (*sensu* Sluijs and Brinkhuis, 2009) (16 %), the *Areoligera-Glaphyrocysta* cpx (8 %), *Operculodinium* spp. (8 %), and *Spiniferites* spp. (6 %). Another important aspect of the palynological assemblage is consistent presence of the freshwater alga *Pediastrum*. The combined information derived from the palynological association and biomarkers therefore implies a near-shore environment with significant river runoff during the latest Paleocene, which is in agreement with the lithological information.

Apectodinium was much more abundant on the GCP in the latest Paleocene (Fig. 2) than at mid- and high latitude sections (e.g., Heilmann-Clausen, 1985; Sluijs et al., 2011). *Apectodinium* was globally abundant during the PETM, suggesting that late Paleocene conditions on the GCP were analogous to those developing on a global scale during the PETM. The ecology of *Apectodinium*, as well as the critical factors triggering its widespread dominance during the PETM remain puzzling. *Apectodinium* tolerated a large salinity range, and likely preferred relatively eutrophic and warm conditions but its global success remains hard to explain (e.g., Sluijs and Brinkhuis, 2009). Upper Paleocene assemblages within the Harrell Core contain 27 % *Apectodinium*, a value close to that recorded at several high-latitude sites during the PETM (Sluijs et al., 2006, 2011). Hence, whatever the critical factor was that triggered the global success of this taxon beginning several kyr prior to the PETM (Sluijs et al., 2007b; Harding et al., 2011), it was likely shared between low and high latitude areas.

CPD
9, 6459–6494, 2013

4.4.2 PETM

By contrast to the upper Paleocene, PETM sediments dominantly yield marine palynomorphs and low BIT values (< 0.1). The concomitant change in lithology from mudstones to glauconite-rich sands and silts indicates sedimentary condensation. Along with dominant *Apectodinium* spp. (between 60 and 85 %), only *Diphyes colligerum* (between 1 and 18 %) and the *Areoligera-Glaphyrocysta* cpx. (3–14 %) are common during the PETM. *Cordosphaeridium fibrospinosum* cpx. and *Spiniferites* spp. (6 %) are consistently present in low abundances. Notably, the *Senegalinium* cpx. and *Eocladopyxis* spp. are mostly absent. The absence of the lagoonal to inner neritic components of the dinocyst assemblage, combined with a massive decrease in the abundance of terrestrial pollen, spores and biomarkers, support an increase in the distance of the site to shore. Common to abundant occurrences of the *Areoligera-Glaphyrocysta* cpx. (here overwhelmed by the *Apectodinium* acme) have also previously been linked to transgression (Iakovleva et al., 2001; Sluijs et al., 2008a). The combined information is consistent with sea level rise during the PETM along the Gulf Coastal Plain. Relative sea level rise is consistent with many marginal marine sedimentary records worldwide (Fig. 1), and indicate PETM-related eustatic rise (Sluijs et al., 2008a).

Previous studies suggested that the Paleocene-Eocene transition was absent from sections along the US margin because of a concurrent drop in sea level (Gibson and Bybell, 1994; Beard, 2008). However, the PETM in this region represents the uppermost part of the Tuscahoma Formation (Harrington, 2003) (Fig. 2). The overlying Bashi Formation has an erosional contact with the Tuscahoma. This suggests that PETM sediments were deposited on the GCP but subsequently eroded in the earliest Eocene. This explains the unconformable upper bound of the PETM in the Harrell core, as described from many other shelf sections worldwide, such as New Jersey and the North Sea (e.g., Sluijs et al., 2008a), as well as the absence of the PETM at many locations along the GCP.

CPD
9, 6459–6494, 2013

4.5 Implications for regional mammal stratigraphy

This sequence stratigraphic scheme has direct implications for inferences regarding primate migrations during the PETM. The discovery of the tiny primate *Teilhardina magnoliana* was reported from the "T4 sand" at the Red Hot Truck Stop (RHTS) (Beard, 2008), which is ~ 10 km north-northeast of the Harrell site. The T4 sand represents the uppermost part of the Tuscahoma Formation at the RHTS, where it resides on top of the glauconitic unit described here to represent the PETM. It was suggested that the T4 sand was deposited during a drop in sea level across the PETM, but this is inconsistent with our data and the position of the T4 sand relative to the glauconitic unit. If the T4 sand was deposited during a drop in sea level, this most likely took place after the PETM, thereby partially reworking material from the PETM. If the T4 sand was indeed deposited during the PETM, which we consider unlikely given the lithological constraints, it was likely deposited within or after the first 80 kyr ("the body") of the event based on our stratigraphic constraints in the Harrell core. However, considering that glauconite-rich sediment accumulation progresses slowly, the deposition of this unite was unlikely restricted to the earliest stage of the PETM, supported by simple probability statistics (Gingerich et al., 2008). This implies that *T. magnoliana* was probably not the earliest primate in North America, which compromises hypothesized migration trajectories as proposed based on that inference (Beard, 2008). Moreover, although regional effects might oppose global sea level trends, the recorded eustatic rise complicates the hypothesis that a drop in sea level facilitated intercontinental mammal migrations during the PETM. More likely, poleward expansion of climate zones set the stage for these migrations (e.g., Bowen et al., 2002).

4.6 Ocean deoxygenation

Within the PETM we recorded sulfur-bound isorenieratane, a derivative of the carotenoid isorenieratene. This chemical fossil is derived from the brown strain of photosynthetic green sulfur bacteria, which requires euxinic (anoxic and sulfidic) conditions

CPD
9, 6459–6494, 2013

(Sinninghe Damsté et al., 1993). It is below the detection limit in the upper Paleocene (Fig. 2). Despite the limited available datapoints, the presence of isorenieratane indicates that photic-zone euxinia developed along the Gulf margin during the PETM. Curiously, while euxinic conditions developed in the photic zone, glauconite was presumably forming on the sea floor, and organic linings of benthic foraminifera (Supplement) are present in the palynological residue, suggesting that the sea floor was oxygenated. The combined information allows for several scenarios to explain this paradox. (1) The lower photic zone but not the sea floor was anoxic. We consider this unlikely because in modern marine environments the sulfide in the water column is almost always formed in the underlying anoxic and sulfidic sediment (e.g., Yao and Millero, 1995). (2) Isorenieratane was transported from euxinic environments further inshore. This mechanism has been proposed previously for other time intervals but is generally considered unlikely (Sinninghe Damsté and Hopmans, 2008) because isorenieratane is among the most labile forms of organic carbon and requires anoxic conditions and short transport time and trajectories to sustain (Harvey, 2006). Hence, it is difficult to envisage that it survived oxic conditions during long-distance transport to the Harrell site. (3) The glauconite and foraminifer linings were transported to the site and concentrated due to sea level rise and sediment starvation, while isorenieratane was produced in the water column at Harrell. This mechanism cannot be excluded with the present data, as detailed sedimentological analyses have not been performed. However, also benthic foraminifer linings are relatively susceptible to oxic degradation. (4) Euxinic conditions developed intermittently. The co-occurrence of benthic fauna and photic zone euxinia in sediments has previously been attributed to decadal or century time-scale variations in water column oxygen concentrations from euxinic to oxygenated both imprinting the sedimentary record (Kenig et al., 2004). Collectively, we consider scenarios 3 and 4 to be the most likely, implying that (intermittent) photic zone euxinia developed at the study site.

These results are consistent with published data from other locations where robust proxy data on seafloor oxygen is available (Fig. 4) (e.g., Dickson et al., 2012).

CPD
9, 6459–6494, 2013

However, while the deep-sea experienced only a limited reduction in seafloor oxygen (Chun et al., 2010), anoxia developed on continental slopes (Nicolo et al., 2010) and shelves (Speijer and Wagner, 2002; Sluijs et al., 2008b). Moreover, at several coastal shelf sites isorenieratane or derivatives thereof have been observed in the sediment, indicating photic zone euxinia (e.g., Sluijs et al., 2006; Fig. 4). In the modern ocean, the presence of isorenieratane in sediments is restricted to semi-enclosed basins, such as the Black Sea. Widespread euxinic conditions also in more oceanic settings have only been previously documented for so-called "global" oceanic anoxic events during the mid-Cretaceous, early Toarcian and at the Permian-Triassic boundary event (e.g., Sinninghe Damsté and Köster, 1998; Grice et al., 2005). Interestingly, these events were also associated with warming and massive perturbations of the global carbon cycle, though the time scales involved were substantially longer than those of the PETM and of anthropogenic changes. The PETM therefore provides the geologically most recent, and likely the best, example of rapidly expanding, widespread, ocean deoxygenation.

Ocean deoxygenation during the PETM was likely generated by processes similar to those contributing to today's so-called "dead zones". Currently, these oxygen depleted zones are caused by coastal eutrophication, stratification and warming resulting from anthropogenic activities (Doney, 2010). If methane originating from submarine hydrates was released at the start of the PETM, its oxidation in the ocean should have caused widespread deoxygenation (Dickens et al., 1997). Ocean circulation may have stagnated at the onset of the event due to changes in climate and the hydrological cycle leading to sea floor O_2 depletion (Ridgwell and Schmidt, 2010; Winguth et al., 2012). Moreover, given the temperature dependence of O_2 solubility in seawater, a rapid $\sim 5\,^{\circ}C$ warming should have decreased O_2 solubility by between 15 and 20 %, depending on the background temperature, which could drive already hypoxic regions to anoxia. Crucially, global warming led to an accelerated hydrological cycle, which together with elevated pCO_2 values resulted in increased weathering (John et al., 2012) and at least regionally seasonal intensification of river runoff (Kopp

CPD
9, 6459–6494, 2013

et al., 2009; Sluijs and Brinkhuis, 2009), leading to increased nutrient input and coastal eutrophication. Importantly, increased SSTs in conjunction with an enhanced hydrological cycle will have strengthened stratification, hampering atmosphere-ocean gas exchange. All these factors, to a different degree, conspired to reduce O_2 concentrations in seawater and allowed for euxinic conditions to develop along coastal margins, although the dominant forcing factor may have been regionally different.

5 PETM continental margin anoxia driven by nutrient feedbacks?

The PETM offers the unique opportunity for the quantification of biogeochemical feedbacks resulting from the rapid expansion of anoxia along continental margins. Similar to what is expected for the future ocean, PETM anoxia likely had major effects on nutrient availability and carbon cycling. Sediments overlain by anoxic bottom waters recycle phosphorus (P) from organic matter efficiently (Slomp and Van Cappellen, 2007). On geological time scales, P is likely the limiting nutrient for marine primary production (Tyrrell, 1999). An increase of anoxia in the global shelf seas would therefore have increased P fluxes and thereby productivity in shelf oceans, as this effect is potentially much larger than that of increased nutrient supply by rivers (Tsandev and Slomp, 2009). Available micropaleontological data, suggesting sustained increased primary productivity in near-shore waters during the PETM (Sluijs et al., 2007a), is consistent with more efficient nutrient cycling. Evidence exists for high rates of nitrogen-fixation (Knies et al., 2008), which may have compensated for nitrogen loss through denitrification and anaerobic ammonium oxidation (anammox) in the low oxygen waters (Kuypers et al., 2005). As proposed for mid-Cretaceous oceanic anoxia (Kuypers et al., 2004), this may have been a dominant factor in sustaining high productivity during the PETM.

The duration of enhanced nutrient cycling and deoxygenation are especially important to assess potential impact on the carbon cycle. Data from most sites point towards anoxia persisting for tens of thousands of years during the PETM (Sluijs et al., 2008b). In part, this may reflect the residence time of the injected carbon that provided the

CPD
9, 6459–6494, 2013

key forcing for the deoxygenation. The residence time of P in the modern ocean is estimated to be between 10 000 and 40 000 yr (Slomp and Van Cappellen, 2007). Although data on absolute P fluxes is lacking, a substantial reduction in the efficiency of P burial in shelf sediments would have increased the residence time of P. This can explain why coastal anoxia persisted for the duration of the body of the PETM, ~ 80 kyr. If this mechanism were active, one would expect high organic carbon burial rates on the shelves during the PETM. Indeed, burial rates of organic carbon significantly increased during the first ~ 80 kyr of the event in many shelf areas (John et al., 2008). Moreover, as sea level rise enlarged the size of the submerged shelves the carbon burial potential increased even further. Even though no climate cooling or recovery of global exogenic $\delta^{13}C$ occurred during this time interval, likely due to continued injection of ^{13}C-depleted carbon (Zeebe et al., 2009), shelves may have represented a significantly enhanced sink of organic carbon during the PETM.

The evolution of ocean oxygen concentrations across the PETM has direct relevance for our understanding of the modern and future ocean. We suggest that the widespread anoxia during the PETM significantly affected nutrient cycles, which in turn acted as an important driver of increased marginal marine productivity and carbon burial. This explains recorded biotic change (Sluijs et al., 2007a), as observed for assemblages of benthic foraminifers, calcareous nannofossils and dinoflagellate cysts. The next challenge is to further quantify the changes in nutrient budgets and oxygen concentrations. This knowledge will help to improve mid- to long-term projections of anthropogenic impacts and the resulting transition towards a warmer, high-CO_2, and low-oxygen ocean.

Supplementary material related to this article is available online at http://www.clim-past-discuss.net/9/6459/2013/cpd-9-6459-2013-supplement.pdf.

CPD
9, 6459–6494, 2013

Acknowledgements. Funding for this research was provided by the Netherlands Organization for Scientific Research (Veni grant 863.07.001 to AS and a Vici grant to SS) and the European Research Council under the European Community's Seventh Framework Program (Starting Grant #259627 to AS and Consolidator Grant #278364 to CS). We thank Paul Markwick for providing the paleogeographic reconstruction, several colleagues including Jerry Dickens (Rice) for comments on an earlier version of this paper, D. Dockery (Office of Geology at the Mississippi Department of Environmental Quality) for access to sediment cores and assistance with sampling, and A. van Dijk, J. van Tongeren, N. Welters (Utrecht University), E. Hopmans, A. Mets and J. Ossebaar (Royal NIOZ) for technical support.

References

Beard, K. C.: The oldest North American primate and mammalian biogeography during the Paleocene–Eocene Thermal Maximum, P. Natl. Acad. Sci. USA, 105, 3815–3818, 2008.

Beard, K. C. and Dawson, M. R.: Early Wasatchian mammals from the Gulf Coastal Plain of Mississippi: biostratigraphic and paleobiogeographic implications, in: Eocene biodiversity: Unusual occurrences and rarely sampled habitats, edited by: Gunnel, G. R., Kluwer Academic/Plenum Publishers, New York, 75–94, 2001.

Bijl, P. K., Schouten, S., Sluijs, A., Reichart, G.-J., Zachos, J. C., and Brinkhuis, H.: Early Palaeogene temperature evolution of the southwest Pacific Ocean, Nature, 461, 776–779, 2009.

Bowen, G. J., Clyde, W. C., Koch, P. L., Ting, S. Y., Alroy, J., Tsubamoto, T., Wang, Y. Q., and Wang, Y.: Mammalian dispersal at the Paleocene/Eocene boundary, Science, 295, 2062–2065, 2002.

Brassell, S. C., Lewis, C. A., de Leeuw, J. W., Lange, F. D., and Sinninghe Damsté, J. S.: Isoprenoid thiophenes: novel products of sediment diagenesis?, Nature, 320, 160–162, 1986.

Brinkhuis, H., Schouten, S., Collinson, M. E., Sluijs, A., Sinninghe Damsté, J. S., Dickens, G. R., Huber, M., Cronin, T. M., Onodera, J., Takahashi, K., Bujak, J. P., Stein, R., van der Burgh, J., Eldrett, J. S., Harding, I. C., Lotter, A. F., Sangiorgi, F., van Konijnenburg-van Cittert, H., de Leeuw, J. W., Matthiessen, J., Backman, J., Moran, K., and Expedition 302 Scientists, T.: Episodic fresh surface waters in the Eocene Arctic Ocean, Nature, 441, 606–609, 2006.

CPD
9, 6459–6494, 2013

Chun, C. O. J., Delaney, M. L., and Zachos, J. C.: Paleoredox changes across the Paleocene-Eocene thermal maximum, Walvis Ridge (ODP Sites 1262, 1263, and 1266): evidence from Mn and U enrichment factors, Paleoceanography, 25, PA4202, doi:10.1029/2009pa001861, 2010.

Danehy, D. R., Wilf, P., and Little, S. A.: Early Eocene Macroflora from the Red Hot Truck Stop Locality (Meridian, Mississippi, USA), Palaeontologia Electronica, 10, 1–31, 2007.

Dickens, G. R.: Down the Rabbit Hole: toward appropriate discussion of methane release from gas hydrate systems during the Paleocene-Eocene thermal maximum and other past hyperthermal events, Clim. Past, 7, 831–846, doi:10.5194/cp-7-831-2011, 2011.

Dickens, G. R., Castillo, M. M., and Walker, J. C. G.: A blast of gas in the latest Paleocene: Simulating first-order effects of massive dissociation of oceanic methane hydrate, Geology, 25, 259–262, 1997.

Dickson, A. J., Cohen, A. S., and Coe, A. L.: Seawater oxygenation during the Paleocene-Eocene Thermal Maximum, Geology, 40, 639–642, 2012.

Doney, S. C.: The growing human footprint on coastal and open-ocean biogeochemistry, Science, 328, 1512–1516, doi:10.1126/science.1185198, 2010.

Dunkley Jones, T., Lunt, D. J., Schmidt, D. N., Ridgwell, A., Sluijs, A., Valdes, P. J., and Maslin, M.: Climate model and proxy data constraints on ocean warming across the Paleocene-Eocene Thermal Maximum, Earth-Sci. Rev., 125, 123–145, doi:10.1016/j.earscirev.2013.07.004, 2013.

Edwards, L. E. and Guex, J.: Graphic correlation of the Marlboro Clay and Nanjemoy Formation (uppermost Paleocene and lower Eocene) of Virginia and Maryland, in: Palynology: Principles and applications, edited by: Jansonius, J. and McGregor, D. C., American Association of Stratigraphic Palynologists Foundation, College Station, Texas, 985–1009, 1996.

Frederiksen, N. O.: Upper Paleocene and lowermost Eocene angiosperm pollen biostratigraphy of the Eastern Gulf Coast and Virginia, Micropaleontology, 44, 45–68, 1998.

Gibbs, S. J., Bown, P. R., Murphy, B. H., Sluijs, A., Edgar, K. M., Pälike, H., Bolton, C. T., and Zachos, J. C.: Scaled biotic disruption during early Eocene global warming events, Biogeosciences, 9, 4679–4688, doi:10.5194/bg-9-4679-2012, 2012.

Gibson, T. G. and Bybell, L. M.: Sedimentary Patterns across the Paleocene-Eocene boundary in the Atlantic and Gulf coastal plains of the United States, Bulletin de la Société Belge de Géologie, 103, 237–265, 1994.

CPD
9, 6459–6494, 2013

Gibson, T. G., Mancini, E. A., and Bybell, L. M.: Paleocene to middle Eocene stratigraphy of Alabama, T. Gulf Coast Assoc. Geol. Soc., 32, 289–294, 1982.
Gingerich, P. D., Rose, K. D., and Smith, T.: Oldest North American primate, P. Natl. Acad. Sci. USA, 105, E30, doi:10.1073/pnas.0802296105, 2008.
Grice, K., Cao, C., Love, G. D., Böttcher, M. E., Twitchett, R. J., Grosjean, E., Summons, R. E., Turgeon, S. C., Dunning, W., and Jin, Y.: Photic Zone Euxinia During the Permian-Triassic Superanoxic Event, Science, 307, 706–709, 2005.
Harding, I. C., Charles, A. J., Marshall, J. E. A., Pälike, H., Roberts, A. P., Wilson, P. A., Jarvis, E., Thorne, R., Morris, E., Moremon, R., Pearce, R. B., and Akbari, S.: Sea-level and salinity fluctuations during the Paleocene-Eocene thermal maximum in Arctic Spitsbergen, Earth Planet. Sc. Lett., 303, 97–107, 2011.
Harland, R.: Dinoflagellate cysts and acritarchs from the Bearpaw Formation (Upper Campanian) of southern Alberta, Canada, Palaeontology, 16, 665–706, 1973.
Harrington, G. J.: Impact of Paleocene/Eocene Greenhouse Warming on North American Paratropical Forests, Palaios, 16, 266–278, 2001.
Harrington, G. J.: Wasatchian (Early Eocene) pollen floras from the Red Hot Truck Stop, Mississippi, USA, Palaeontology, 46, 725–738, 2003.
Harrington, G. J. and Jaramillo, C. A.: Paratropical floral extinction in the Late Palaeocene-Early Eocene, Palaeontology, 46, 725–738, 2007.
Harrington, G. J., Kemp, S. J., and Koch, P. L.: Palaeocene-Eocene paratropical floral change in North America: Responses to climate change and plant immigration, J. Geol. Soc. London, 161, 173–184, 2004.
Harvey, H. R.: Sources and cycling of organic matter in the marine water column, in: Marine Organic Matter, The Handbook of Environmental Chemistry, 2N, edited by: Volkman, J. K., Springer, Berlin, Germany, 1–25, 2006.
Heilmann-Clausen, C.: Dinoflagellate stratigraphy of the Uppermost Danian to Ypresian in the Viborg 1 borehole, Central Jylland, Denmark, DGU A7, 1–69, 1985.
Hopmans, E. C., Weijers, J. W. H., Schefuß, E., Herfort, L., Sinninghe Damsté, J. S., and Schouten, S.: A novel proxy for terrestrial organic matter in sediments based on branched and isoprenoid tetraether lipids, Earth Planet. Sc. Lett., 224, 107–116, 2004.
Huber, M. and Caballero, R.: The early Eocene equable climate problem revisited, Clim. Past, 7, 603–633, doi:10.5194/cp-7-603-2011, 2011.

CPD
9, 6459–6494, 2013

Huguet, C., De Lange, G. J., Middelburg, J. J., Sinninghe Damsté, J. S., and Schouten, S.: Selective preservation of soil organic matter in oxidized marine sediments (Madeira Abyssal Plain), Geochim. Cosmochim. Acta, 72, 6061–6068, 2008.

Iakovleva, A. I., Brinkhuis, H., and Cavagnetto, C.: Late Palaeocene-Early Eocene dinoflagellate cysts from the Turgay Strait, Kazakhstan; correlations across ancient seaways, Palaeogeogr. Palaeocl., 172, 243–268, 2001.

John, C. M., Bohaty, S. M., Zachos, J. C., Sluijs, A., Gibbs, S. J., Brinkhuis, H., and Bralower, T. J.: North American continental margin records of the Paleocene-Eocene thermal maximum: implications for global carbon and hydrological cycling, Paleoceanography, 23, PA2217, doi:10.1029/2007PA001465, 2008.

John, C. M., Banerjee, N. R., Longstaffe, F. J., Sica, C., Law, K. R., and Zachos, J. C.: Clay assemblage and oxygen isotopic constraints on the weathering response to the Paleocene-Eocene thermal maximum, east coast of North America, Geology, 40, 591–594, doi:10.1130/g32785.1, 2012.

Keating-Bitonti, C. R., Ivany, L. C., Affek, H. P., Douglas, P., and Samson, S. D.: Warm, not super-hot, temperatures in the early Eocene subtropics, Geology, 39, 771–774, 2011.

Kenig, F., Hudson, J. D., Sinninghe Damsté, J. S., and Popp, B. N.: Intermittent euxinia: reconciliation of a Jurassic black shale with its biofacies, Geology, 32, 421–424, 2004.

Kennett, J. P. and Stott, L. D.: Abrupt deep-sea warming, palaeoceanographic changes and benthic extinctions at the end of the Palaeocene, Nature, 353, 225–229, 1991.

Kim, J.-H., van der Meer, J., Schouten, S., Helmke, P., Willmott, V., Sangiorgi, F., Koç, N., Hopmans, E. C., and Sinninghe Damsté, J. S.: New indices and calibrations derived from the distribution of crenarchaeal isoprenoid tetraether lipids: implications for past sea surface temperature reconstructions, Geochim. Cosmochim. Acta, 74, 4639–4654, 2010.

Knies, J., Mann, U., Popp, B. N., Stein, R., and Brumsack, H.-J.: Surface water productivity and paleoceanographic implications in the Cenozoic Arctic Ocean, Paleoceanography, 23, PA1S16, doi:10.1029/2007pa001455, 2008.

Kopp, R. E., Schumann, D., Raub, T. D., Powars, D. S., Godfrey, L. V., Swanson-Hysell, N. L., Maloof, A. C., and Vali, H.: An Appalachian Amazon? Magnetofossil evidence for the development of a tropical river-like system in the mid-Atlantic United States during the Paleocene-Eocene thermal maximum, Paleoceanography, 24, PA4211, doi:10.1029/2009pa001783, 2009.

CPD
9, 6459–6494, 2013

Kuypers, M. M. M., van Breugel, Y., Schouten, S., Erba, E., and Damsté, J. S. S.: N2-fixing cyanobacteria supplied nutrient N for Cretaceous oceanic anoxic events, Geology, 32, 853–856, doi:10.1130/g20458.1, 2004.

Kuypers, M. M. M., Lavik, G., Woebken, D., Schmid, M., Fuchs, B. M., Amann, R., Jørgensen, B. B., and Jetten, M. S. M.: Massive nitrogen loss from the Benguela upwelling system through anaerobic ammonium oxidation, P. Natl. Acad. Sci. USA, 102, 6478–6483, doi:10.1073/pnas.0502088102, 2005.

Lourens, L. J., Sluijs, A., Kroon, D., Zachos, J. C., Thomas, E., Röhl, U., Bowles, J., and Raffi, I.: Astronomical pacing of late Palaeocene to early Eocene global warming events, Nature, 435, 1083–1087, 2005.

Lunt, D. J., Dunkley Jones, T., Heinemann, M., Huber, M., LeGrande, A., Winguth, A., Loptson, C., Marotzke, J., Roberts, C. D., Tindall, J., Valdes, P., and Winguth, C.: A model–data comparison for a multi-model ensemble of early Eocene atmosphere–ocean simulations: EoMIP, Clim. Past, 8, 1717–1736, doi:10.5194/cp-8-1717-2012, 2012.

Mancini, E. A.: Lithostratigraphy and biostratigraphy of Paleocene subsurface strata in southwest Alabama, T. Gulf Coast Assoc. Geol. Soc., 31, 359–367, 1981.

Mancini, E. A.: Biostratigraphy of Paleocene strata in southwestern Alabama, Micropaleontology, 30, 268–291, 1984.

Mancini, E. A. and Oliver, G. E.: Planktic foraminifers from the Tuscahoma Sand (upper Paleocene) of southwest Alabama, Micropaleontology, 27, 204–225, 1981.

Mancini, E. A. and Tew, B. H.: Geochronology, biostratigraphy, and sequence stratigraphy of a marginal marine shelf stratigraphic succession: Upper Paleocene and Lower Eocene, Wilcox Group, eastern Gulf Coast plain, USA, in: Geochronology, time scales and global stratigraphic correlation, edited by: Berggren, W. A., Kent, D. V., Aubry, M.-P., and Hardenbol, J., SEPM (Society of Sedimentary Geology) Special Publication, 54, 281–293, 1995.

Markwick, P. J.: The palaeogeographic and palaeoclimatic significance of climate proxies for data-model comparisons, in: Deep-Time Perspectives on Climate Change: Marrying the Signal from Computer Models and Biological Proxies, edited by: Williams, M. A. M. H., Gregory, F. J., and Schmidt, D. N., The Micropalaeontological Society Special Publications, The Geological Society, London, 2007.

Martini, E.: Standard Tertiary and Quaternary calcareous nannoplankton zonation, in: Proceedings of the II Planktonic Conference, Roma 1970, Vol. 2, edited by: Farinacci, A., Edizioni Tecnoscienza, Rome, 739–785, 1971.

CPD
9, 6459–6494, 2013

McCarren, H., Thomas, E., Hasegawa, T., Röhl, U., and Zachos, J. C.: Depth dependency of the Paleocene-Eocene carbon isotope excursion: paired benthic and terrestrial biomarker records (Ocean Drilling Program Leg 208, Walvis Ridge), Geochem. Geophy. Geosy., 9, Q10008, doi:10.1029/2008GC002116, 2009.

McInerney, F. A. and Wing, S. L.: The Paleocene-Eocene Thermal Maximum: a perturbation of carbon cycle, climate, and biosphere with implications for the future, Ann. Rev. Earth Planet. Sci., 39, 489–516, 2011.

Nicolo, M. J., Dickens, G. R., and Hollis, C. J.: South Pacific intermediate water oxygen depletion at the onset of the Paleocene-Eocene Thermal Maximum as depicted in New Zealand margin sections, Paleoceanography, 25, PA4210, doi:10.1029/2009PA001904, 2010.

Peterse, F., Kim, J.-H., Schouten, S., Kristensen, D. K., Koç, N., and Sinninghe Damsté, J. S.: Constraints on the application of the MBT/CBT palaeothermometer at high latitude environments (Svalbard, Norway), Org. Geochem., 40, 692–699, 2009.

Peterse, F., van der Meer, J., Schouten, S., Weijers, J. W. H., Fierer, N., Jackson, R. B., Kim, J. H., and Sinninghe Damsté, J. S.: Revised calibration of the MBT/CBT paleotemperature proxy based on branched tetraether membrane lipids in surface soils, Geochim. Cosmochim. Acta, 96, 215–229, 2012.

Rhodes, G. M., Ali, J. R., Hailwood, E. A., King, C., and Gibson, T. G.: Magnetostratigraphic correlation of Paleogene sequences from northwest Europe and North America, Geology, 28, 927–930, 1999.

Ridgwell, A. and Schmidt, D. N.: Past constraints on the vulnerability of marine calcifiers to massive carbon dioxide release, Nat. Geosci., 3, 196–200, 2010.

Schoon, P. L., Sluijs, A., Sinninghe Damsté, J. S., and Schouten, S.: High productivity and elevated carbon isotope fractionations in the Arctic Ocean during Eocene Thermal Maximum 2, Paleoceanography, 26, PA3215, doi:10.1029/2010PA002028, 2011.

Schouten, S., Huguet, C., Hopmans, E. C., Kienhuis, M. V. M., and Sinninghe Damsté, J. S.: Analytical methodology for TEX86 paleothermometry by high-performance liquid chromatography/atmospheric pressure chemical ionization-mass spectrometry, Anal. Chem., 79, 2940–2944, 2007.

Sessa, J. A., Bralower, T. J., Patzkowsky, M. E., Handley, J. C., and Ivany, L. C.: Environmental and biological controls on the diversification and ecological reorganization of Late Cretaceous and early Paleogene marine ecosystems in the Gulf Coastal Plain, Paleobiology, 38, 218–239, 2012a.

CPD
9, 6459–6494, 2013

Sessa, J. A., Ivany, L. C., Schlossnagle, T. H., Samson, S. D., and Schellenberg, S. A.: The fidelity of oxygen and strontium isotope values from shallow shelf settings: implications for temperature and age reconstructions, Palaeogeogr. Palaeocl., 342–343, 27–39, 2012b.

Siesser, W. G.: Paleogene calcareous nannoplankton biostratigraphy: Mississippi, Alabama and Tennessee, Mississippi Department of Natural Resources Bureau of Geology Bulletin, 125, 1–61, 1983.

Sinninghe Damsté, J. S. and Hopmans, E. C.: Does fossil pigment and DNA data from Mediterranean sediments invalidate the use of green sulfur bacterial pigments and their diagenetic derivatives as proxies for the assessment of past photic zone euxinia?, Environ. Microbiol., 10, 1392–1399, doi:10.1111/j.1462-2920.2008.01609.x, 2008.

Sinninghe Damsté, J. S. and Köster, J.: A euxinic southern North Atlantic Ocean during the Cenomanian/Turonian oceanic anoxic event, Earth Planet. Sc. Lett., 158, 165–173, 1998.

Sinninghe Damsté, J. S., Rijpstra, W. I. C., Leeuw, J. W. D., and Schenk, P. A.: Origin of organic sulphur compounds and sulphur-containing high molecular weight substances in sediments and immature crude oils, Org. Geochem., 13, 593–606, 1988.

Sinninghe Damsté, J. S., Wakeham, S. G., Kohnen, M. E. L., Hayes, J. M., and de Leeuw, J. W.: A 6,000-year sedimentary molecular record of chemocline excursions in the Black Sea, Nature, 362, 827–829, 1993.

Slomp, C. P. and Van Cappellen, P.: The global marine phosphorus cycle: sensitivity to oceanic circulation, Biogeosciences, 4, 155–171, doi:10.5194/bg-4-155-2007, 2007.

Sluijs, A. and Brinkhuis, H.: A dynamic climate and ecosystem state during the Paleocene-Eocene Thermal Maximum: inferences from dinoflagellate cyst assemblages on the New Jersey Shelf, Biogeosciences, 6, 1755–1781, doi:10.5194/bg-6-1755-2009, 2009.

Sluijs, A. and Dickens, G. R.: Assessing offsets between the $\delta^{13}C$ of sedimentary components and the global exogenic carbon pool across Early Paleogene carbon cycle perturbations, Global Biogeochem. Cy., 26, GB4005, doi:10.1029/2011GB004224, 2012.

Sluijs, A., Schouten, S., Pagani, M., Woltering, M., Brinkhuis, H., Sinninghe Damsté, J. S., Dickens, G. R., Huber, M., Reichart, G.-J., Stein, R., Matthiessen, J., Lourens, L. J., Pedentchouk, N., Backman, J., Moran, K., and The Expedition 302 Scientists: Subtropical Arctic Ocean temperatures during the Palaeocene/Eocene thermal maximum, Nature, 441, 610–613, 2006.

Sluijs, A., Bowen, G. J., Brinkhuis, H., Lourens, L. J., and Thomas, E.: The Palaeocene-Eocene thermal maximum super greenhouse: biotic and geochemical signatures, age models and

CPD
9, 6459–6494, 2013

mechanisms of global change, in: Deep Time Perspectives on Climate Change: Marrying the Signal from Computer Models and Biological Proxies, edited by: Williams, M., Haywood, A. M., Gregory, F. J., and Schmidt, D. N., The Micropalaeontological Society, Special Publications, The Geological Society London, London, 323–347, 2007a.

Sluijs, A., Brinkhuis, H., Schouten, S., Bohaty, S. M., John, C. M., Zachos, J. C., Reichart, G.-J., Sinninghe Damsté, J. S., Crouch, E. M., and Dickens, G. R.: Environmental precursors to light carbon input at the Paleocene/Eocene boundary, Nature, 450, 1218–1221, 2007b.

Sluijs, A., Brinkhuis, H., Crouch, E. M., John, C. M., Handley, L., Munsterman, D., Bohaty, S. M., Zachos, J. C., Reichart, G.-J., Schouten, S., Pancost, R. D., Sinninghe Damsté, J. S., Welters, N. L. D., Lotter, A. F., and Dickens, G. R.: Eustatic variations during the Paleocene-Eocene greenhouse world, Paleoceanography, 23, PA4216, doi:10.1029/2008PA001615, 2008a.

Sluijs, A., Röhl, U., Schouten, S., Brumsack, H.-J., Sangiorgi, F., Sinninghe Damsté, J. S., and Brinkhuis, H.: Arctic late Paleocene–early Eocene paleoenvironments with special emphasis on the Paleocene-Eocene thermal maximum (Lomonosov Ridge, Integrated Ocean Drilling Program Expedition 302), Paleoceanography, 23, PA1S11, doi:10.1029/2007PA001495, 2008b.

Sluijs, A., Schouten, S., Donders, T. H., Schoon, P. L., Röhl, U., Reichart, G. J., Sangiorgi, F., Kim, J.-H., Sinninghe Damsté, J. S., and Brinkhuis, H.: Warm and wet conditions in the Arctic region during Eocene Thermal Maximum 2, Nat. Geosci., 2, 777–780, 2009.

Sluijs, A., Bijl, P. K., Schouten, S., Röhl, U., Reichart, G.-J., and Brinkhuis, H.: Southern ocean warming, sea level and hydrological change during the Paleocene-Eocene thermal maximum, Clim. Past, 7, 47–61, doi:10.5194/cp-7-47-2011, 2011.

Speijer, R. P. and Wagner, T.: Sea-level changes and black shales associated with the late Paleocene thermal maximum: organic-geochemical and micropaleontologic evidence from the southern Tethyan margin (Egypt-Israel), Geol. Soc. Am. Spec. Pap., 356, 533–549, 2002.

Taylor, K. W. R., Huber, M., Hollis, C. J., Hernandez-Sanchez, M. T., and Pancost, R. D.: Re-evaluating modern and Palaeogene GDGT distributions: implications for SST reconstructions, Global Planet. Change, 108, 158–174, doi:10.1016/j.gloplacha.2013.06.011, 2013.

Thomas, E.: Starvation, Asphyxiation, Eutrophication and Dissolution: Killing Benthic Foraminifera at the End of the Paleocene, 8th Internation Conference on Paleoceanogrphy; An Ocean View of Global Change, Biarritz, France, 2004.

CPD
9, 6459–6494, 2013

Thomas, E. and Shackleton, N. J.: The Palaeocene-Eocene benthic foraminiferal extinction and stable isotope anomalies, in: Correlation of the Early Paleogene in Northwestern Europe, Geological Society London Special Publication 101, edited by: Knox, R. W. O. B., Corfield, R. M., and Dunay, R. E., Geological Society of London, London, UK, 401–441, 1996.

Thomas, E. and Zachos, J. C.: Was the late Paleocene thermal maximum a unique event?, Geologiska Föreningens i Stockholm Förhandlingar, GFF, Transactions of the Geological Society in Stockholm, 122, 169–170, 2000.

Thrasher, B. L. and Sloan, L. C.: Carbon dioxide and the early Eocene climate of western North America, Geology, 37, 807–810, 2009.

Tsandev, I. and Slomp, C. P.: Modeling phosphorus cycling and carbon burial during Cretaceous Oceanic Anoxic Events, Earth Planet. Sc. Lett., 286, 71–79, 2009.

Tschudy, R. H.: Stratigraphic distribution of significant Eocene palynomorphs of the Mississippi Embayment, US Geological Survey Professional Paper 743-B, US Geological Survey, United States Government Printing Office, Washington, 1973.

Tyrrell, T.: The relative influences of nitrogen and phosphorus on oceanic primary production, Nature, 400, 525–531, 1999.

Vandenberghe, N., Speijer, R. P., and Hilgen, F. J.: The Paleogene Period, in: The Geologic Time Scale 2012, edited by: Gradstein, F. M., Ogg, J. G., Schmitz, M., and Ogg, G., Elsevier, 855–921, 2012.

Volkman, J. K.: A review of sterol markers for marine and terrigenous organic matter, Org. Geochem., 9, 83–99, 1986.

Wade, B. S., Pearson, P. N., Berggren, W. A., and Pälike, H.: Review and revision of Cenozoic tropical planktonic foraminiferal biostratigraphy and calibration to the geomagnetic polarity and astronomical time scale, Earth-Sci. Rev., 104, 111–142, doi:10.1016/j.earscirev.2010.09.003, 2011.

Weijers, J. W. H., Schouten, S., Spaargaren, O. C., and Sinninghe Damsté, J. S.: Occurrence and distribution of tetraether membrane lipids in soils: implications for the use of the TEX86 proxy and the BIT index, Org. Geochem., 37, 1680–1693, 2006.

Weijers, J. W. H., Schouten, S., van den Donker, J. C., Hopmans, E. C., and Sinninghe Damste, J. S.: Environmental controls on bacterial tetraether membrane lipid distribution in soils, Geochim. Cosmochim. Acta, 71, 703–713, 2007.

Wing, S. L. and Currano, E. D.: Plant response to a global greenhouse event 56 million years ago, Am. J. Bot., 100, 1234–1254, 2013.

CPD
9, 6459–6494, 2013

Wing, S. L., Harrington, G. J., Smith, F. A., Bloch, J. I., Boyer, D. M., and Freeman, K. H.: Transient floral change and rapid global warming at the Paleocene-Eocene boundary, Science, 310, 993–996, doi:10.1126/science.1116913, 2005.

Winguth, A. M. E., Thomas, E., and Winguth, C.: Global decline in ocean ventilation, oxygenation, and productivity during the Paleocene-Eocene Thermal Maximum: implications for the benthic extinction, Geology, 40, 263–266, doi:10.1130/g32529.1, 2012.

Wolfe, J. A. and Dilcher, D. L.: Late Paleocene through Middle Eocene climates in lowland North America, Geologiska Föreningens i Stockholm Förhandlingar, GFF; Transactions of the Geological Society in Stockholm, 122, 184–185, 2000.

Yao, W. and Millero, F. J.: The chemistry of the anoxic waters in the Framvaren Fjord, Norway, Aquat. Geochem., 1, 53–88, 1995.

Zachos, J. C., Wara, M. W., Bohaty, S., Delaney, M. L., Petrizzo, M. R., Brill, A., Bralower, T. J., and Premoli Silva, I.: A transient rise in tropical sea surface temperature during the Paleocene-Eocene thermal maximum, Science, 302, 1551–1554, 2003.

Zachos, J. C., Schouten, S., Bohaty, S., Quattlebaum, T., Sluijs, A., Brinkhuis, H., Gibbs, S., and Bralower, T. J.: Extreme warming of mid-latitude coastal ocean during the Paleocene-Eocene Thermal Maximum: inferences from TEX86 and Isotope Data, Geology, 34, 737–740, 2006.

Zachos, J. C., Dickens, G. R., and Zeebe, R. E.: An early Cenozoic perspective on greenhouse warming and carbon-cycle dynamics, Nature, 451, 279–283, 2008.

Zeebe, R. E., Zachos, J. C., and Dickens, G. R.: Carbon dioxide forcing alone insufficient to explain Palaeocene-Eocene Thermal Maximum warming, Nat. Geosci., 2, 576–580, 2009.

Zonneveld, K. A. F., Marret, F., Versteegh, G. J. M., Bogus, K., Bonnet, S., Bouimetarhan, I., Crouch, E., de Vernal, A., Elshanawany, R., Edwards, L., Esper, O., Forke, S., Grøsfjeld, K., Henry, M., Holzwarth, U., Kielt, J.-F. ß., Kim, S.-Y., Ladouceur, S. P., Ledu, D., Chen, L., Limoges, A., Londeix, L., Lu, S. H., Mahmoud, M. S., Marino, G., Matsouka, K., Matthiessen, J., Mildenhal, D. C., Mudie, P., Neil, H. L., Pospelova, V., Qi, Y., Radi, T., Richerol, T., Rochon, A., Sangiorgi, F., Solignac, S., Turon, J.-L., Verleye, T., Wang, Y., Wang, Z., and Young, M.: Atlas of modern dinoflagellate cyst distribution based on 2405 data points, Rev. Palaeobot. Palynol., 191, 1–197, doi:10.1016/j.revpalbo.2012.08.003, 2013.

CPD
9, 6459–6494, 2013

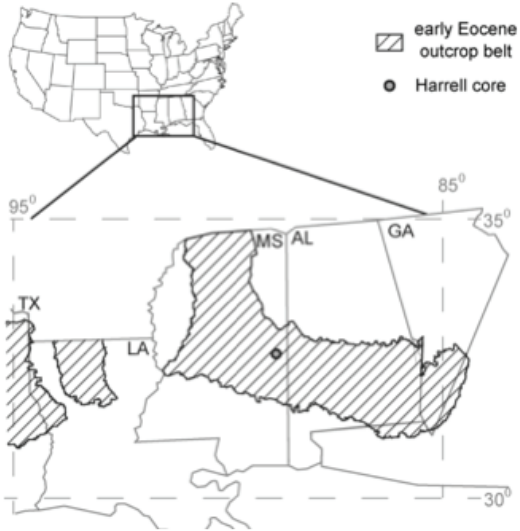

Fig. 1. Location map of the Harrell Core in Lauderdale Co., Mississippi, USA and outcrop belt of early Eocene marginal marine deposits along the eastern Gulf of Mexico. Diagram was modified from Sessa et al. (2012b).

CPD
9, 6459–6494, 2013

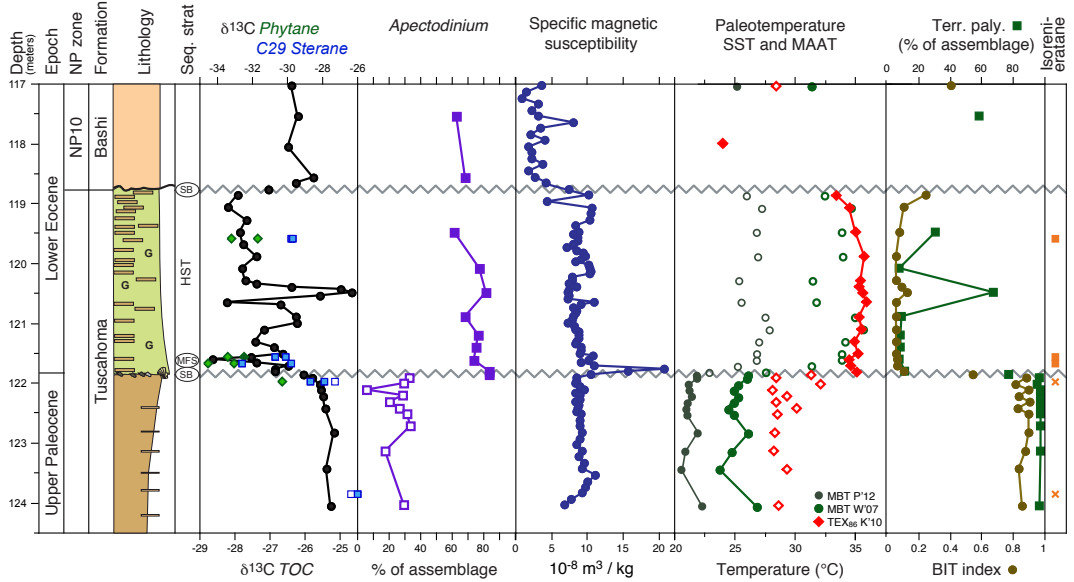

Fig. 2. Paleontological and geochemical records across the PETM in the Harrell Core. Lithological units represent upper Paleocene organic rich heterogenous, locally laminated mudstones (brown); PETM glauconitic (G) sands and silts (green) and early Eocene siliciclastics with carbonate (light brown). Light-colored and open symbols in the $\delta^{13}C$ values of sulfur-bound phytane, and sulfur-bound C_{29} sterane yield a relatively high uncertainty of ~ 1 and 1.5 ‰ in isotope values, respectively, due to the low abundance of these compounds in the sediments. Upper Paleocene *Apectodinium* abundances (open squares) should be considered rough estimates; average Paleocene values are 27 % (see text and Supplement). Calibration-related errors on absolute temperatures for TEX_{86} and MBT/CBT temperatures are 2.5 and 5 °C, respectively. Open TEX_{86} (diamonds) and MBT (circles) symbols indicate temperatures that may be biased by high supply of terrestrial lipids or in situ production, respectively (see text). Crosses at isorenieratane indicate intervals where this biomarker is below detection limits.

CPD
9, 6459–6494, 2013

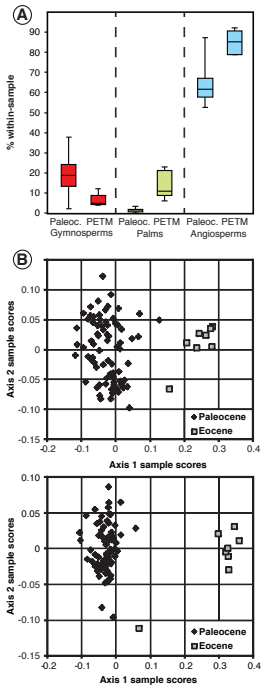

Fig. 3. Pollen and spore results. **(A)** Box-plot comparisons between average (mean) within-sample abundance of pre-PETM samples ($n = 77$) from Harrington and Jaramillo (2007) and PETM samples ($n = 8$) from the Tuscahoma Formation of the Harrell Core. Abundances are expressed as average percent within-sample. All comparisons between pre-PETM abundances and PETM abundances are statistically significant. **(B)** Non-metric multidimensional scaling illustrating pollen compositional differences in the Tuscahoma Formation in the Harrell Core, based on the relative abundance data (top panel) on presence absence data of (bottom panel). While the former reflects changes in dominant taxa, the latter is sensitive to changes in the co-occurrence patterns of taxa within samples.

CPD
9, 6459–6494, 2013

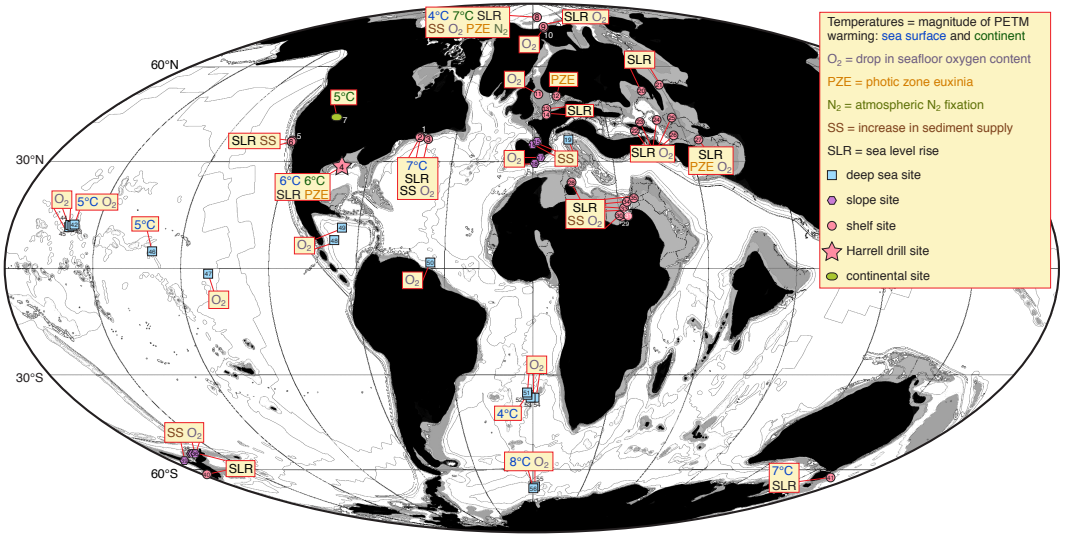

Fig. 4. Records of relative changes in SST (blue), continental MAAT (green), decreases in sea floor O_2 content (O_2), photic zone euxinia (PZE), atmospheric nitrogen fixation, sea level rise (SLR) and increasing siliciclastic sediment supply (SS) on a paleogeographic map (modified from Markwick, 2007) during the PETM. Star indicates the location of the Harrell Core. See Supplement for site information and the nature and source of the data.

CPD
9, 6459–6494, 2013